



# Environmentally Assisted Cracking: Science and Engineering

Lisagor/Crooker/  
Leis, editors



STP 1049



**STP 1049**

# ***Environmentally Assisted Cracking: Science and Engineering***

*W. Barry Lisagor, Thomas W. Crooker, and Brian N. Leis, editors*



ASTM  
1916 Race Street  
Philadelphia, PA 19103

## Library of Congress Cataloging-in-Publication Data

Environmentally assisted cracking: science and engineering / W. Barry Lisagor, Thomas W. Crooker, and Brian N. Leis, editors.  
(STP : 1049)

Proceedings of the ASTM Symposium on Environmentally Assisted Cracking: Science and Engineering, held Nov. 9-11, 1987, Bal Harbour, Fla., sponsored by ASTM Committees G-1 on Corrosion of Metals, E-24 on Fracture Testing, and E-9 on Fatigue.

Includes bibliographical references.

"ASTM publication code number (PCN) 04-010490-30"—T.p. verso.  
ISBN 0-8031-1276-9

1. Metals—Fracture—Environmental aspects—Congresses.
2. Alloys—Fracture—Environmental aspects—Congresses.
3. Metals—Cracking—Environmental aspects—Congresses.

I. Lisagor, W. Barry. II. Crooker, T. W. III. Leis, B. N. IV. ASTM Symposium on Environmentally Assisted Cracking: Science and Engineering (1987: Bal Harbour, Fla.) V. American Society for Testing and Materials. Committee G-1 on Corrosion of Metals. VI. ASTM Committee E-24 on Fracture Testing. VII. ASTM Committee E-9 on Fatigue.  
TA460.E495 1990  
620.1'66—dc20

89-18581  
CIP

Copyright © by AMERICAN SOCIETY FOR TESTING AND MATERIALS 1990

### NOTE

The Society is not responsible, as a body,  
for the statements and opinions  
advanced in this publication.

### Peer Review Policy

Each paper published in this volume was evaluated by three peer reviewers. The authors addressed all of the reviewers' comments to the satisfaction of both the technical editor(s) and the ASTM Committee on Publications. —

The quality of the papers in this publication reflects not only the obvious efforts of the authors and the technical editor(s), but also the work of these peer reviewers. The ASTM Committee on Publications acknowledges with appreciation their dedication and contribution of time and effort on behalf of ASTM.

## Foreword

The ASTM Symposium on Environmentally Assisted Cracking: Science and Engineering was held in Bal Harbour, Florida, on 9–11 Nov. 1987. The event was sponsored by ASTM Committees G-1 on Corrosion of Metals, E-24 on Fracture Testing, and E-9 on Fatigue. The symposium chairmen were W. B. Lisagor and T. W. Crooker of the National Aeronautics and Space Administration, and B. N. Leis of Battelle Columbus Laboratories. This publication was edited by Mr. Lisagor, together with Messrs. Crooker and Leis.

# Contents

<b>Overview</b>	1
 <b>MECHANISMS</b>	
<b>Influence of Strain on Hydrogen Assisted Cracking of Cathodically Polarized High-Strength Steel—J. R. SCULLY AND P. J. MORAN</b>	5
Discussion	29
<b>Thermomechanical Treatments and Hydrogen Embrittlement of Ferritic Stainless Steels with Different Interstitial Contents—R. N. IYER, R. F. HEHEMANN, AND A. R. TROIANO</b>	30
<b>Influence of Overload and Temperature on Stress Corrosion Crack Growth Behavior in a Low-Alloy Steel—V. VENUGOPAL AND S. K. PUTATUNDA</b>	42
<b>Role of the Oxide Film in the Transgranular Stress Corrosion Cracking of Copper—T. B. CASSAGNE, J. KRUGER, AND E. N. PUGH</b>	59
Discussion	75
<b>Coherency Stress and Transgranular Stress Corrosion Cracking of Cu–18Au Alloy—J. D. FRITZ, B. W. PARKS, AND H. W. PICKERING</b>	76
<b>Role of Selective Dissolution in Transgranular Stress-Corrosion Cracking: Studies of Transient and Steady-State Dealloying in Copper-Gold Alloys—W. F. FLANAGAN, J. B. LEE, D. MASSINON, M. ZHU, AND B. D. LICHTER</b>	86
 <b>MATERIAL PERFORMANCE—I</b>	
<b>Effects of Electrochemical Potential on the Slow Strain Rate Fracture of 4340 Steel in a Combustion Product Residue—R. D. DANIELS, A. P. SADARANGANI, M. S. MAGNER, AND K. J. KENNELLEY</b>	103
<b>Environmental Acceleration of Fatigue Crack Growth in Reactor Pressure Vessel Materials and Environments—W. A. VAN DER SLUYS AND R. H. EMANUELSON</b>	117

<b>Interactive Effects of Cold Work, Yield Strength, and Temperature on Sulfide Stress Cracking—M. W. JOOSTEN, J. J. MURALI, AND J. L. HESS</b>	136
---	-----

<b>Sensitivity to Sulfide-Stress Cracking at Welds in Line-Pipe Steels—H. J. CIALONE AND D. N. WILLIAMS</b>	152
Discussion	167

<b>Factors Affecting the Susceptibility of Carbon-Manganese Steel Welds to Cracking in Sour Environments—R. J. PARGETER</b>	169
---	-----

## MODELING AND ANALYSIS

<b>A Mechanics-Based Analysis of Stress-Corrosion Cracking of Line-Pipe Steel in a Carbonate-Bicarbonate Environment—B. N. LEIS AND W. J. WALSH</b>	243
---	-----

<b>A Model for Environmentally Assisted Crack Growth Rate—G. GABETTA, C. RINALDI, AND D. POZZI</b>	266
--	-----

<b>Modeling of Sulfide Inclusion Distributions in Relation to the Environmentally Assisted Cracking of Low-Alloy Steels in a Pressurized Water Reactor Environment—D. I. SWAN AND O. J. V. CHAPMAN</b>	283
--	-----

## MATERIAL PERFORMANCE—II

<b>Effects of Stress and Stress History on the Magnitude of the Environmental Attack in Renè 80—S. J. BALSONE, T. NICHOLAS, AND M. KHOBAIB</b>	303
--	-----

<b>Role of Environment in Elevated Temperature Crack Growth Behavior of Renè N4 Single Crystal—M. KHOBAIB, T. NICHOLAS, AND S. V. RAM</b>	319
---	-----

<b>Environmental and Microstructural Influence on Fatigue Propagation of Small Surface Cracks—J. PETIT AND A. ZEGHLOUL</b>	334
--	-----

<b>Environmentally Induced Fatigue Crack Propagation Under Variations in the Loading Conditions—K. SCHULTE, H. NOWACK AND G. LÜTJERING</b>	347
--	-----

<b>Environmental Influence on the Effect of a Single Overload on the Fatigue Crack Growth Behavior on a High-Strength Aluminum Alloy—N. RANGANATHAN, M. QUINTARD, J. PETIT, AND J. DE FOUQUET</b>	374
---	-----

## TEST METHODS

<b>Evaluation of <math>K_{ISCC}</math> and <math>da/dt</math> Measurements for Aluminum Alloys Using Precracked Specimens—M. S. DOMACK</b>	393
--	-----

<b>Influence of Experimental Variables on the Measurement of Stress Corrosion Cracking Properties of High-Strength Steels—</b> R. W. JUDY, JR., W. E. KING, JR., J. A. HAUSER II, AND T. W. CROOKER	410
 MATERIAL PERFORMANCE—III	
<b>Keyhole Compact Tension Specimen Fatigue of Selected High-Strength Steels in Seawater—</b> S. S. RAJPATHAK AND W. H. HARTT	425
<b>Cyclic Tension Corrosion Fatigue of High-Strength Steels in Seawater—</b> W. J. D. JONES AND A. P. BLACKIE	447
<b>Fatigue Crack Growth Behavior of Different Stainless Steels in Pressurized Water Reactor Environments—</b> C. AMZALLAG AND J-L. MAILLARD	463
<b>Environmentally Assisted Cracking Behavior of a High-Level Nuclear Waste Container Alloy—</b> L. A. JAMES AND D. R. DUNCAN	495
<b>Corrosion Fatigue Cracking of Chromium-Containing Steels—</b> B. D. HARTY AND R. E. J. NOËL	505
<b>Evaluation of Cavitation-Erosion Resistance of Ion-Plated Titanium Nitride Coating—</b> M. MATSUMURA, Y. OKA, R. EBARA, T. KOBAYASHI, T. ODOHIRA, T. WADA, AND M. HATANO	521
<b>Author Index</b>	535
<b>Subject Index</b>	537

# Overview

---

The Symposium on Environmentally Assisted Cracking: Science and Engineering was organized to assess progress in the understanding and control of this phenomenon, recognized as one of the most serious causes of structural failure over a broad range of industrial application. This mode of failure continues to pose a long-term concern for the use of metallic materials in applications involving aggressive liquid and gaseous environments throughout the range of service temperatures. Research into environmentally assisted cracking has continued to progress in recent years. ASTM has previously held a series of symposia on various aspects of this phenomenon, most recently in April 1982 (see ASTM STP 821). With the continuing research on this important cause of metal failure and new service applications placing increasing demands on metallic structures, the organizers from ASTM Committees G-1, E-24, and E-9 recognized the need for another broad-based symposium addressing both the science and the engineering aspects of the subject. The resulting symposium was held 9–11 November 1987 in Bal Harbour, Florida.

Papers were solicited on a range of topics that included phenomena, basic mechanisms, modeling, test methodologies, materials performance, engineering applications, and service experience and failures. This volume reflects the current emphasis with regard to material/environment systems, research community addressing the topic, and specific technical interest. The content suggests that the subject continues to cover the broad spectrum of structural alloys and environments as well as numerous test methods and approaches.

As a result of the invited presentations, the symposium was organized into six sessions, including sessions addressing mechanisms, modeling and analysis, and test methods; and three sessions addressing material performance to specific service environments. It is anticipated that a greater appreciation of all aspects of this complex phenomenon, mechanical as well as chemical and electrochemical and their interaction, will be derived from the information presented; and that no single preferred test technique or concept will likely emerge in the future but that all will contribute to a better understanding of materials behavior.

The editors would like to acknowledge other members of the symposium Organizing Committee who contributed to the content of the symposium as well as this publication and who served as chairmen of various symposium sessions. They include: D. O. Sprowls, Committee G-1; R. P. Gangloff, Committee E-24; and C. Q. Bowles, Committee E-9. We would also like to extend sincere appreciation to the ASTM staff, both technical and editorial, for their diligent efforts in the conduct of the symposium and the preparation of this publication.

## *W. Barry Lisagor*

Head, Metallic Materials Branch NASA  
Langley Research Center, Hampton, VA;  
symposium chairman and editor.

## *Thomas W. Crooker*

National Aeronautics and Space Administration,  
Washington, DC; symposium chairman and editor.

## *Brian N. Leis*

Battelle Columbus Labs., Columbus, OH;  
symposium chairman and editor.





## **Mechanisms**



# Influence of Strain on Hydrogen Assisted Cracking of Cathodically Polarized High-Strength Steel

---

**REFERENCE:** Scully, J. R. and Moran, P. J., "Influence of Strain on Hydrogen Assisted Cracking of Cathodically Polarized High-Strength Steel," *Environmentally Assisted Cracking: Science and Engineering*, ASTM STP 1049, W. B. Lisagor, T. W. Crooker, and B. N. Leis, Eds., American Society for Testing and Materials, Philadelphia, 1990, pp. 5–29.

**ABSTRACT:** Evidence is presented that confirms the role of mechanical strain in promoting surface absorption of hydrogen in two high strength steels under cathodic polarization in alkaline 3.5% sodium chloride solution. Data are reported for a 5Ni-Cr-Mo-V steel {896 MPa (130 ksi) yield strength} and is compared to data previously developed for AISI 4340 steel {1207 MPa (175 ksi) yield strength}. Strain induced bare surface generation is shown to substantially influence both alloys' hydrogen cracking susceptibility. Strain enhanced absorption is empirically observed for tensile specimens under slowly straining conditions and is also suggested to explain the hydrogen assisted cracking behavior of slowly strained DCB compact and cantilever beam fracture mechanics specimens with pre-existing fatigue cracks. Enhancement of hydrogen absorption per unit area of bare surface, as determined by straining hydrogen permeation measurements, explain the effect. In the presence of a corroded surface, the kinetics of the hydrogen evolution reaction are modified such that a lower cathodic hydrogen overpotential is observed at a given cathodic current density. This lowers hydrogen absorption at a given applied cathodic current density. Hydrogen permeation rates are increased upon straining independent of changes in the apparent bulk diffusion coefficient. These findings indicate that sustained plus cyclic loading and low-cycle fatigue of steels in seawater are more severe environmental cracking conditions than sustained loading typical of laboratory cantilever beam tests.

**KEY WORDS:** cracking, environmental effects, adsorption, absorption, diffusion, corrosion, cathodic protection, cyclic loading, dislocation transport, fatigue (materials), film rupture, embrittlement, high strength steel, hydrogen, hydrogen embrittlement, hydrogen evolution, hydrogen permeation, seawater, stress corrosion cracking, sustained load, threshold stress intensity, trapping

The hydrogen assisted cracking of high-strength steels in sodium chloride solution has been shown to proceed in four distinct stages [1–4]. These include an incubation stage, cracking initiation, crack propagation, and crack arrest. During incubation, solution transport to the crack tip or pre-existing flaw, electrochemical reaction, hydrogen adsorption, hydrogen absorption, hydrogen diffusion, and hydrogen segregation occur. Cracking initiation in the case of high strength steels occurs in the triaxially stressed region at the position

<sup>1</sup> Senior member of Technical Staff, Metallurgy Department, Sandia National Laboratories, Albuquerque, NM 87158; formerly, The David Taylor Naval Ship Research and Development Center, Annapolis, MD.

<sup>2</sup> Associate professor, Corrosion and Electrochemistry Research Laboratory, Department of Materials Science and Engineering, The Johns Hopkins University, Baltimore, MD 21218.

of stress concentration where a certain state of stress and segregated hydrogen content simultaneously exist [5]. The threshold stress intensity,  $K_{th}$ , for hydrogen cracking initiation has been linked directly with the estimated subsurface hydrogen concentration,  $C_0$  [6–8] through an inverse power law relationship. Under sustained load, dead weight load, or increasing load conditions, hydrogen cracking initiation may temporarily lead to crack arrest or transition to ductile crack propagation as increasing stress intensities promote crack advance into a zone of material initially containing a lower segregated hydrogen content. In the case of a fixed initial crack opening displacement or constant strain, crack advance eventually decreases the operative stress intensity thereby promoting crack arrest. In either case, after crack arrest, additional hydrogen accumulation may satisfy the original criteria for initiation (certain state of stress and certain critical segregated hydrogen content) and the process may repeat. Thus initiation may be considered a key step in the overall hydrogen assisted cracking process for high-strength steels undergoing environmental hydrogen cracking phenomena.

Resistance to the initiation of environmental cracking can be characterized by  $K_{Isc}$ , or  $K_{th}$ , the threshold stress intensity for environmental cracking. At applied stress intensities above this value crack propagation occurs. Empirically  $K_{th}$  has been found to vary from 10 to 75% of the inert environment fracture toughness,  $K_{Ic}$  [7]. In fact, both  $K_{th}$  and Region II crack growth rates have been found to be strongly dependent on the following factors for a particular alloy and heat treatment: load rate or strain rate [9–11], prior levels of applied Mode I crack tip stress intensity [12–16], the frequency of the applied delta  $K$ , applied delta  $K$  magnitude, applied delta  $K$  waveform [17–20], the localized environmental composition and impurity level [2,3,21], and the crack tip electrode potential [22–24]. Explanations for such noted variability in  $K_{th}$  or Region II crack growth rates have usually relied upon the slow kinetics of one of the discrete sequential steps in the hydrogen accumulation process [25,26]. Many quantitative kinetic models for hydrogen assisted cracking of high-strength steels assume hydrogen diffusion to be the rate limiting process for crack growth [16,27–32]. Dislocation enhanced transport of hydrogen has been postulated [33,34] and investigated as a means of enhancing hydrogen permeation and accumulation [35–46]. The role of surface strain in enhancing hydrogen cracking phenomena through modification of surface absorption has not been thoroughly considered.

Recent work [11] showed a strong influence of the crosshead displacement rate (and crack tip strain rate) on the hydrogen assisted cracking susceptibility of pre-cracked AISI 4340 steel in 3.5% sodium chloride (NaCl) solution. The strain rate (displacement rate) was found to have a strong influence on the threshold stress-intensity value for hydrogen cracking independent of the extent of precharging. Particularly, lower strain rates promoted increased susceptibility and consequently lower-threshold stress-intensity values. Conversely, the extent of precharging under slight load had very little influence on the critical stress intensity value at the higher strain rate. One interpretation of these results is that the increasing stress intensity and crack tip strain ruptures surface films at the crack tip exposing fresh metal surface to the solution which enhances hydrogen absorption. Surface films have been found to alter hydrogen absorption for iron in alkaline chloride solutions [47–50]. The lower strain rate utilized in the study cited previously [11] may have allowed sufficient time after film rupture for hydrogen absorption, transport, and subsequent embrittlement of a zone of material in front of the crack tip. Faster strain rates not only rupture films, but promote rapid increases in the stress intensity, causing ductile crack propagation prior to adequate hydrogen absorption, transport, and segregation. Fractography supported this scenario with the lower strain rate results exhibiting intergranular cracking at prior austenite grain boundaries for a distance that ranged from 400 to 1000  $\mu\text{m}$  ahead of the initial air fatigue crack

tip. The fast strain rate tests exhibited only ductile fracture that was also typical for the air tests.

This hypothesis was confirmed by additional studies on AISI 4340 [51,52]. In these tests, straining hydrogen permeation experiments and other slow strain rate studies with and without prior corrosion film formation confirmed that hydrogen absorption rates were enhanced when the corroded surface was either ruptured by straining or avoided in surface preparation. Decreases in ductility were observed when straining and cathodic polarization were applied concurrently.

Strain enhanced absorption may also explain the increased hydrogen embrittlement susceptibility observed in several other studies of steels in seawater under sustained plus cyclic loading or low cycle fatigue [17–20]. All of these studies are linked by the presence of concurrent strain and cathodic polarization in cases where hydrogen damage was maximized. Here, we investigate 5Ni-0.5Cr-0.5Mo-0.05V steel similar in microstructure, composition, and strength to AISI 4340. It has been shown that the hydrogen cracking susceptibility of this steel under cathodic polarization in seawater was markedly increased by high  $R$  ratio, low frequency, cyclic loading or low cycle fatigue [18].

Here, we confirm the feasibility of the hydrogen absorption hypothesis developed above for the 5Ni-0.5Cr-0.5Mo alloy. Extensive comparison of experimental results to those obtained for AISI 4340 steel are made.

## Experimental Procedures

### *Materials and Specimen Preparation*

Samples were produced from single heats of either 5Ni-0.5Cr-0.5Mo-0.05V steel (Mil-S-24371A), or AISI 4340 steel (UNS No. G43400), both heat treated to form tempered martensite. The AISI 4340 alloy is the identical heat of AISI 4340 utilized in the fracture work described previously [11]. This alloy had a nominal yield strength of 1207 MPa (175 ksi), 10 to 12% elongation, and 40 to 50% reduction in area at failure in air. The 5Ni-0.5Cr-0.5Mo-0.05V steel (Mil-S-24371A) alloy was produced with a 896 MPa (130 ksi) yield strength, 19 to 22% elongation in 5 cm (2 in.) and a 65 to 80% reduction in area at failure in air. Nominal compositions are given in Table 1.

TABLE 1—Nominal composition (in percent by weight) of AISI 4340 steel and 5Ni-Cr-Mo-V steel.

Element	5Ni-Cr-Mo-V <sup>a</sup>	AISI 4340 <sup>b</sup>
Fe	BAL	BAL
C	0.13	0.41
Mn	0.82	0.74
P	...	0.009
S	0.002	0.016
Si	0.24	0.21
Cu	0.05	...
Ni	5.20	2.00
Cr	0.44	0.74
Mo	0.52	0.26
V	0.05	0.05
Ti	...	...
Material code	FYP	FYS

<sup>a</sup> Composition determined by: ladle analysis.

<sup>b</sup> Composition determined by commercial laboratory analysis.

*Environments*

All electrolytes employed in this study were prepared from reagent grade chemicals and deionized water (5 to 12  $\mu\text{S}/\text{cm}$  conductivity). Electrolytes were 0.6 M NaCl adjusted to a specific pH in the range of 8 to 11 with sodium hydroxide (NaOH), or ASTM artificial ocean water at a pH of 8.2 to 8.4 [53]. The alkaline chloride environment was chosen to simulate the conditions created in the occluded crack tip environment of a steel alloy when under the application of external cathodic polarization in a neutral chloride environment. Such conditions have been clearly demonstrated in the literature [22–24,54–57]. All experiments were conducted at a temperature of between 24 and 27°C.

*Slow Strain Rate Tests*

Three different types of slow strain rate samples were utilized; smooth, tapered hourglass, and notched. Details are illustrated in Fig. 1. Notched samples were utilized to promote greater strain localization, strain rates, and stress intensification upon loading qualitatively approaching that of the crack tip region of the double cantilever beam specimen of previous studies [11,18]. All slow strain rate specimens were oriented with the tensile axis perpendicular to the rolling direction of the plate.

Tests were performed at displacement rates ranging from  $2.54 \times 10^{-7}$  to  $2.54 \times 10^{-2}$  cm/s ( $10^{-7}$  to  $10^{-2}$  in./s). This produced engineering strain rates of  $10^{-7}$  to  $10^{-2}$  s $^{-1}$  for the smooth 1 in. gage length samples (prior to necking). The reduction in cross sectional area of the specimen at failure or maximum load or both during test were determined. From the method described by Bueckner [58] the stress-intensity factor at the breaking load was estimated. Given the notch sensitivity of the AISI 4340 alloy, in particular, this stress intensity was considered to be representative of the threshold stress intensity,  $K_{th}$ , for cracking initiation at the particular cathodic charging level. During straining, specimens were cathod-

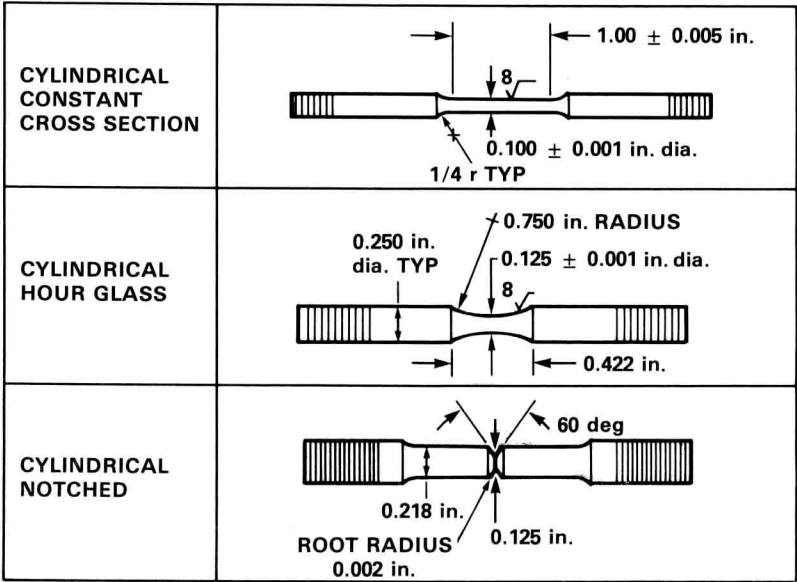


FIG. 1—Slow strain rate test specimen types and dimensions.

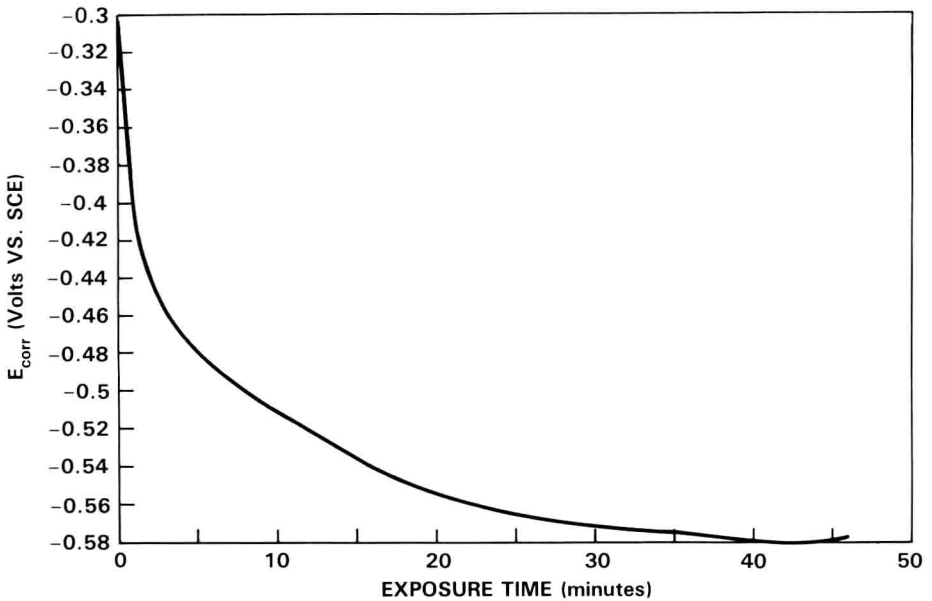


FIG. 2—Transient open circuit potential behavior for polished 5Ni-Cr-Mo-V steel in ASTM artificial ocean water.

ically polarized under potentiostatic control. Other details concerning specimen preparation and testing procedures have been previously discussed [51].

All samples were initially exposed at open circuit for a period of less than several minutes. The open circuit potential behavior obtained upon exposure is illustrated in Fig. 2. Using the impedance method, an initial corrosion rate of 40 to 50  $\mu\text{A}/\text{cm}^2$  was estimated. A corrosion film replaced the air formed oxide on all slow strain rate specimens during this period prior to cathodic polarization. This condition was considered to be representative of, for instance, a precracked or notched region of metal under sustained (but not cyclic) load with creep strains only, before cathodic polarization, hydrogen cracking initiation, and exposure to bare metal. Even after cathodic polarization ohmic resistance may limit the initial level of cathodic current at the crack tip under static loading. Subsequent cyclic loading has been shown to produce order of magnitude increases in cathodic currents in addition to increasing crack tip strain [59].

#### Hydrogen Permeation Studies

The Devanathan-Stachurski technique [60] was utilized to study hydrogen permeation. In all cases the cathodic charging side was controlled at a constant current. These current densities utilized ranged from  $-30$  to  $-1200 \mu\text{A}/\text{cm}^2$  depending upon experiment (in ASTM convention cathodic currents and current densities are considered negative). The cathodic current densities in the low end of this range (near  $-30 \mu\text{A}/\text{cm}^2$ ) are representative of cathodic protection current densities actually observed per unit area of bare sections of cathodically polarized steel in seawater. As mentioned, transient current increases with strain can far exceed these current densities [59]. Electroless and sputter deposited palladium coated exit surfaces were utilized in all cases. Exit surfaces were potentiostatically controlled



in a potential ranging from  $-550$  to  $-650$  mV versus SCE. This potential was sufficiently negative to minimize anodic currents arising from steel dissolution should the palladium be ruptured in the straining experiment. Background current densities of less than  $-0.1$  and  $-0.4$   $\mu\text{A}/\text{cm}^2$  were obtained in static and straining Devanathan-Stachurski experiments, respectively. In the case of straining experiments, preliminary experiments confirmed that this background current remained cathodic during the period of straining. This background level was subtracted from the exit anodic current density as is the normal procedure. One group of Devanathan-Stachurski experiments was conducted with the specimen instantaneously cathodically polarized while the electrolyte was added. In this manner, oxidation of the surface in the chloride containing electrolyte was avoided (or minimized). This method has been previously discussed [51,52] and is hereafter referred to as instantaneous cathodic polarization, or ICP. Other samples experienced some prior anodic dissolution by corrosion at potentials ranging from  $-400$  to  $-650$  mV versus SCE, consistent with the results shown in Fig. 2 for periods ranging from seconds to hours. Hereafter, this condition will be called slightly corroded.

Specimens were strained at a constant extension rate of  $11.43 \times 10^{-7}$  cm/s ( $4.5 \times 10^{-7}$  in./s) ( $4.5 \times 10^{-7}$  s $^{-1}$  nominal engineering strain rate) or  $2 \times 10^{-6}$  s $^{-1}$  to a total strain not exceeding uniform macroscopic plastic elongation (that is, below the ultimate engineering tensile strength and before the onset of necking). Concerning cyclic straining, the constant extension rate was reversed for time periods of 200 min per cycle. Results are presented for nominally identical test runs conducted in alkaline 0.6 M sodium chloride solution at a cathodic galvanostatic charging current density of  $-500$   $\mu\text{A}/\text{cm}^2$ . The transient permeation rise and decay method previously discussed [52,61] provided direct means to verify that the permeation increases reported in Table 2 are not artifacts of background current changes but truly represent increases in the hydrogen permeation rate.

The kinetics of the water reduction reaction were investigated for both steels during the nonstraining permeation experiments under the same conditions described above. Hydrogen overpotentials for the water reduction reaction were determined from measurements of the working to reference electrode potential taking into consideration the measured solution pH.

## Results

### *Slow Strain Rate Tests: Influence of Strain Rate*

Figures 3 and 4 illustrate the effects of strain rate at constant cathodic polarization levels for smooth AISI 4340 and 5Ni-Cr-Mo-V steel alloy samples, respectively. The data are presented as percent reduction in area at failure versus strain rate. The reversible potential for the reduction of water in ASTM ocean water is  $-0.74$  V versus SCE. Therefore  $-0.85$  V versus SCE (Fig. 3) is a lower overpotential relative to the  $-1.00$  V versus SCE polarization level possible for structures cathodically polarized in seawater with zinc sacrificial anodes [22,51,55,56]. For AISI 4340 steel hydrogen susceptibility is observed at strain rates below approximately  $10^{-4}$  for the  $-1.00$  V level and at lower strain rates for the  $-0.85$  V level. Concerning the AISI 4340 steel alloy at  $-1.00$  V versus SCE, the percent reduction in area decreases from 45% at a strain rate of  $10^{-4}$  or greater to 10% at a strain rate of  $10^{-5}$  or less. Similar behavior is observed at  $-0.85$  V versus SCE except that the percent reduction in area is less substantially reduced at the intermediate and lower strain rates. For the 5Ni-Cr-Mo-V steel alloy, qualitatively similar behavior is observed with the percent reduction in area decreasing from greater than 45% at  $10^{-4}$  s $^{-1}$  to below 20% at a  $3 \times 10^{-7}$  strain rate at  $-1.00$  V versus SCE.

Figures 5 and 6 illustrate the influence of displacement rate on embrittlement susceptibility